Peganum Harmala Extract as an Eco-Friendly Corrosion Inhibitor for Carbon Steel N80 in 1 M HCl: Electrochemical and Surface Morphological Studies

Ali Khabar Aksh[1], Adnan Sultan Abdul Nabi[1], Hadi Thamer Obaid[2]

[1]Department of Chemistry, College of Education for Pure Sciences, Basrah University, Basrah, Iraq
[2]Department of Medical Physics, College of Applied Medical Science, Shatrah University, Thi-Qar, Iraq
Email: pgs.ali.kh@uobasrah.edu.iq

By utilizing surface examination and electrochemical strategies, the review tries to determine the level of inhibitory efficacy of Peganum Harmala aqueous extract on the corrosion of N80 carbon steel alloy, which is used in the oil pipe industry, in 1 Molar HCl solution at various temperatures and inhibitor concentrations. Due to the thicker protective layer, the inhibitor's efficacy was demonstrated by the results, which also showed that the inhibitor's inhibitory efficacy increased as its concentration did. At a concentration of 200 ppm and a temperature of 298 K, the maximum inhibitory efficiency of 91.26% was achieved.

When the plant inhibitor is present, the corrosion rate (CR) drops. When the inhibitor was not employed, the corrosion rate (CR) in the acidic medium (HCl 1M) was 15.58 mpy; however, due to the inhibitor's effect on the current density Icorr, the CR decreased to 1.36 mpy. As a result of adding the inhibitor, the corrosion current density of N80 carbon steel dropped from 34.22 µA/cm² for the sample without inhibitor to 2.99 µA/cm² for the sample with 200 ppm of the used plant inhibitor, according to the polarization data.

The corrosion inhibitor is of the blended type, meaning it hinders both cathodic and anodic processes, as per the electrochemical analysis and polarization curves. The thin coating that the inhibitor created on the carbon steel alloy's surface to prevent corrosion was identified using scanning electron microscopy (SEM). FT-IR analysis of the inhibitor's chemical structure indicated the presence of heteroatoms and functional groups in it.

Keywords: Corrosion, plant extract, polarization curves, carbon steel, corrosion protection.

1. Introduction

One of the main issues facing the oil and gas industry's transportation and production sectors

is carbon steel corrosion, which accounts for 25% of failures and puts human life and the environment at risk from natural gas and oil leaks [1]. With the development of industrial technologies, new problems regarding corrosion constantly appear that require finding effective methods of protection. Due to the different nature and types of corrosion that can occur and also the different conditions that help these different types to occur, it necessitates the use of several methods to protect against corrosion. There are four basic ways to combat and protect against corrosion, where corrosion is controlled by taking specific measures. These measures may relate to the metals and alloys used in terms of their selection and method of use, or to the medium or environment to which these materials are exposed in terms of interference with some of the environmental factors affecting corrosion. Furthermore, these procedures involve applying specific electrochemical methods to protect materials externally, and combining two or more of these methods results in effective corrosion control [2]. With high demand for crude oil to increase profits, due to their operating environment, researchers are racing to develop green corrosion inhibitors (plant extracts) that are effective at high temperatures, inexpensive, environmentally friendly, non-toxic, and provide a high rate of inhibition efficiency [3]. The components can be easily extracted in very simple ways, so these products are compatible with humans and the environment [4]. The extract of natural products contains many organic molecules that contain aromatic rings or functional groups such as hydroxyl, carbonyl, carboxyl, 2NH, CO, and CHO atoms. Adsorbed on the metal surface are heterogeneous compounds that inhibit corrosion, like O, N, S, P, and triple bonds. These compounds create a protective layer. In acidic settings, this kind of inhibitor is employed [5][6][7]. The herb employed in this study, Harmala seeds, or scientifically known as Peganum harmala, is endemic to the arid region extending from northern India to the eastern Mediterranean and is extensively distributed throughout Iran. Different alkaloids with various structures found in P. harmala are challenging to synthesise. On the other hand, the extract of the ripe fruit or blossom contains a variety of active alkaloids, particularly beta-carboline, including harmalol, harmaline, and harmine, as well as structurally simpler compounds. It is a perennial plant [8]. The experimental portion will be examined in the section that follows.

2. The Experimental Part

In this part, first, the researchers will examine the chemicals and devices that are going to be used.

2.1 Chemicals and devices used

We ordered chemicals and solvents from BDH, and the SiC2 silicon carbide paper and Harmal seeds were sourced from the local market. N-80 carbon steel alloy was supplied by SOC. Infrared spectra were measured using an FT-IR-8400S Fourier Transform Infrared spectrometer in the laboratories of the University of Tehran, Islamic Republic of Iran. To identify the chemicals present in the plants, a gas chromatography-mass spectrophotometer (GC-MS) with a 5973 Network Mass Selective Detector was utilized, also at the University of Tehran.

Additionally, a solvent called DMSO-d6 was employed. Furthermore, the Bank Elektronik

Insightful Controls Type M lab 200, Germany (2007), was used for additional applications. This study aims to measure the corrosion rate of the N80 carbon steel alloy. The morphological changes on the surface of the carbon steel composite were observed using a scanning electron microscope (SEM) at the University of Tehran. The composition of the carbon steel alloy components is detailed in Table 1. Moreover, various combinations were used in the study.

2.2 Alloys used

In this study, carbon steel alloy (Carbon Steel N-80) prepared by the South Oil Company was used. Table (1) shows the proportions of the components of this alloy [9].

Table 1: Composition of the Carbon Steel Alloy

Element	Fe	S	P	C	Mn
Percentage (%)	98.39	0.06	0.05	0.3	1.2

2.3 Preparation of Corrosion Solution

The corrosion solution was prepared from concentrated hydrochloric acid (HCl) at a concentration of (1M) by the dilution method.

2.4 Preparation of Peganum Harmala extract

Peganum Harmala fruit is a readily available and inexpensive fruit in the Iraqi markets. It is taken and ground well, then the extraction process is carried out by weighing (10 gm) of Peganum Harmala powder and adding (300 ml) of deionized water in a (500 ml) glass beaker. It is then heated to 70°C for (30 min) in the presence of a mechanical stirrer. The solution is then left to cool for two hours, then filtered using filter paper, and the filtrate is taken and dried at 50°C for 48 hours. This resulted in a dry powder weighing 1.5 gm. The standard extract is then ready by dissolving (1 gm) of the extract in (1000 ml) of refined water in a one-liter volumetric carafe, coming about in a (1000 ppm) standard arrangement. A progression of various fixations were then pre-arranged utilizing the weakening condition [10].

2.5 Measuring the speed of corrosion

The speed of the corrosion was done by the electrochemical method by (Tafel Plot Extrapolation). This method was used to measure the corrosion rate. It is considered a modern, advanced, and relatively economical method in terms of the time required for the experiment and the metal sample used. The sample is connected to an electrochemical cell, which is in turn connected to a device that provides all the information needed about corrosion. This information is displayed in curves on the screen of the computer connected to the device. The curves are plotted directly using an icon on the screen that represents the change in the logarithm of the current (I). The gadget comprises chiefly of the estimating cell, which contains three terminals: The functioning cathode, which is set in the example utilized; The helper cathode, which is made of platinum; The reference anode, which is a calomel anode. This method involves measuring the corrosion current, corrosion potential, and plotting a Tafel plot. After cleaning and preparing the sample (a piece of clean carbon

steel alloy), it is connected to the working electrode and inserted into the test cell. The auxiliary and reference electrodes are placed in the same cell after filling it with the appropriate volume of (1M) hydrochloric acid solution. The cell is then connected to the device and the required information is entered, including the start and end voltage and the process time. The device then outputs the results in the form of a graph (Tafel plot). The device is then turned off, the contents of the cell are emptied and cleaned, and the process is repeated using a clean carbon steel alloy. The cell is then refilled with the corrosive solution and different concentrations of the inhibitor are added. The measurement is then repeated [11].

3. Results and Discussion

In this section, the results of the experiments carried out will be presented as well as their discussions.

3.1 Fourier transform infrared (FTIR)

Adsorption of inhibitors to safeguard the metal surface is the essential stage in corrosion hindrance. To reveal a few insight into expected connections between the adsorbed inhibitor and the carbon steel surface in the acidic HCI 1M climate with plant extract, FT-IR examination is done. The inhibitor's synthetic construction decides areas of strength for how hindrance is. caramel (R) seed extract portrayal to evaluate the essential useful gatherings. The infrared spectra's outcomes are shown in Table (2) and Figure (1), though Table (2) features the critical groups for the extract R.

Table (2): Values of infrared spectral frequencies in (cm-1) for the plant extract (R)

υ(O-H)	υ(C-H)$_{ali}$	υ(N-H)	υ(C=O)	υ(CH2)	υ(C-O) ast	υ(C-N)	υ(C-Br)	υ(C=N)
3300	2939	3205	1649	1454	1205	1051	638	1629
(C-H) arm	υ (C=C)	υ (N=N)	(C-O) Est	υ (NH2)	υ (C-H) ali			
3192	1575	1440	1132	3292	2939			

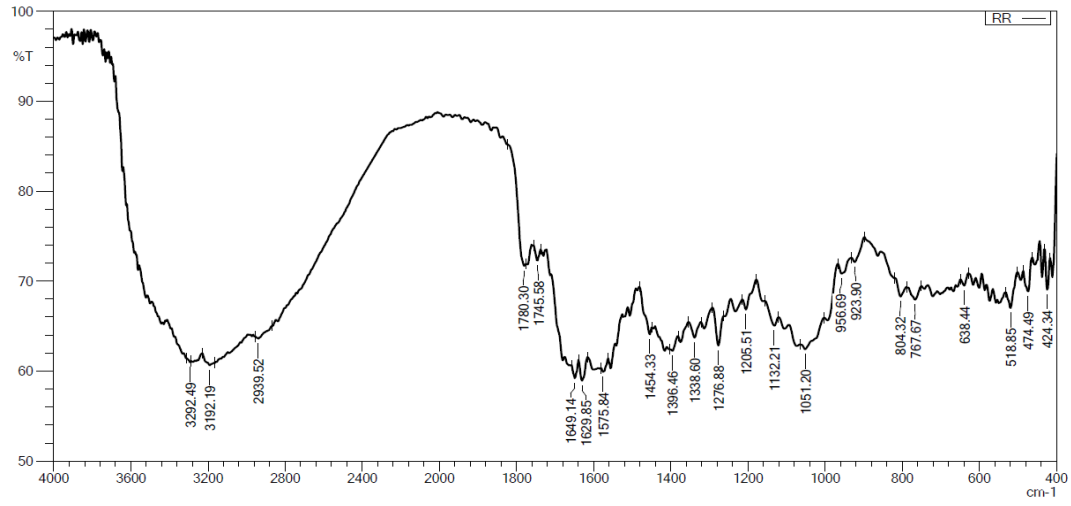

Figure (1): Infrared spectrum of the inhibitor (R)

3.2 Mass- Spectrum Extracted Plant (GC – mass)

The researchers recorded the GC-MASS spectra for the plant extract (R) to identify the chemical compounds that explain its inhibitory mechanism. Table 3 represents the most important components that appeared in the plant inhibitor (R). The mass spectrum of extract R is shown in Figure 2.

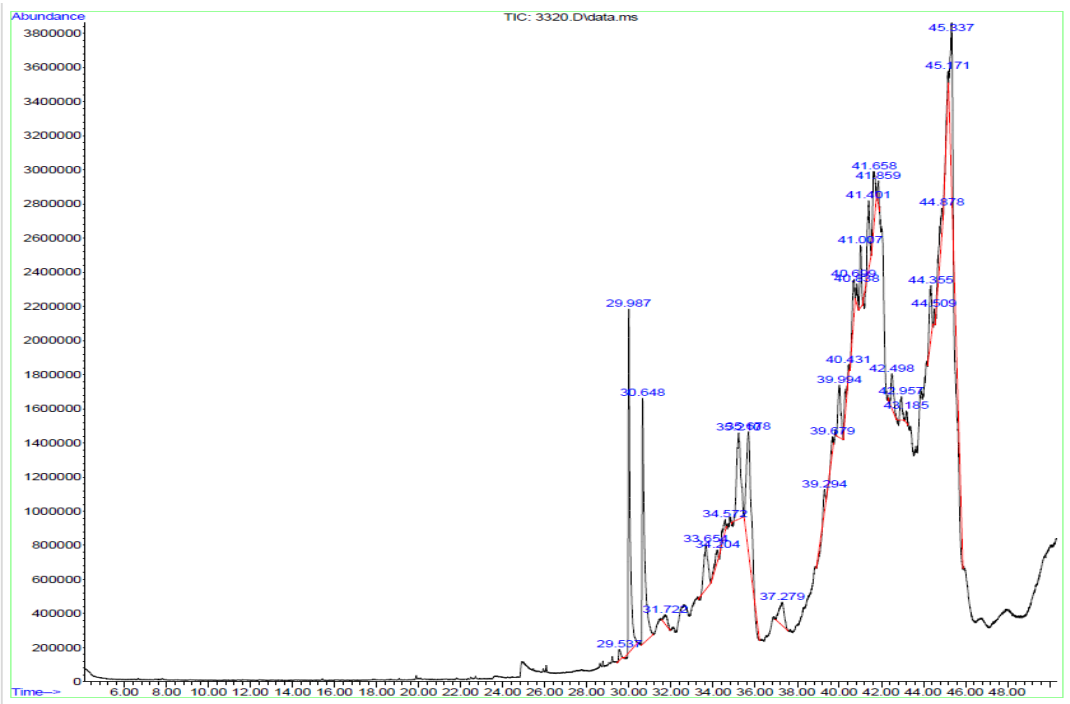

Figure (2) represents the mass spectrum of the aqueous extract of plant (R)

Table (3). shows the most important components that appeared in the plant inhibitor (R)

Number	RT (min)	Area %	Name	Quality	CAS Number
1	29.537	0.59	Hexahydrofluorene, 3-methoxy-6-methyl-	91	000000-00-0
2	29.989	16.65	Harmaline	95	000304-21-2
3	30.647	16.04	Harmine	98	000442-51-3
4	33.652	29.19	Glycerol 2-acetate 1,3-dipalmitate	64	118656-09-0
5	40.433	1.21	dimethyl 3,4:5,6-dibenzocarbazol-1,8-dicarboxylate	58	000000-00-0
6	40.433	15.61	Oleic acid, eicosyl ester	58	000000-00-0
7	35.675	14.20	8H-dibenzo[a,g]quinolizin-8-one, 5,6-dihydro-2,3-dimethoxy-13-phenyl	64	015495-36-0
8	34.202	1.12	Methyl 3-(4-Azido-2,3,5,6-tetrafluorobenzamido)-5-aminobenzoate	43	000000-00-0

3.3 Utilizing the integral polarization strategy, the viability of the watery extract as a corrosion inhibitor of carbon steel was explored at temperatures (298, 308, 318 K) with and without the plant inhibitor and at focuses (50, 100, 150, and 200 ppm). The medium used for the study was an acidic 1 M aqueous solution of HCl acid. The study's findings revealed the following:

(a) Polarization curves, or so-called Tafel lines

The way of the anodic and cathodic responses that were utilized to concentrate on it utilizing the electrochemical technique (polarization bend strategy) in the nonattendance and presence of various centralizations of the concentrated on plant extract not entirely set in stone to all the more likely figure out the job of the watery extract (R), which is utilized as an inhibitor of the corrosion cycle of carbon steel. It yielded the upsides of the cathodic (βc) and anodic (βa) Tafel constants, as well as the corrosion voltage (E corr) and current thickness (I corr). Because plant inhibitors (R) tend to slow down the reaction at both the anode and the cathode in the same way, adding varying amounts of them didn't significantly alter the Tafel curve's form, as seen in Figures 3-5 and Table 4. This indicates that the reaction was impacted by the inhibitors. Because the reaction is both cathodic and anodic, it is a mixed type [12]. This indicates that the anodic reaction is hampered and the cathode reaction's release of hydrogen gas is delayed when an inhibitor is added to the acidic solution. Inhibitor C decreases the quantity of active reaction sites involved in the corrosion reaction by

adsorbing on the metal surface [13]. The researchers found that the Tafel curve's shape largely stays the same when the inhibitor R is added at various concentrations. This is due to the fact that the inhibitors often exhibit a nearly equal reduction in response at the anode and cathode electrodes, suggesting that they are of the mixed kind. Equation can be used to get the inhibitory efficiency percentage (IE%) (1) [14]:

$$\% \text{ IE} = \left(\frac{\text{I°corr} - \text{Icorr}}{\text{I°corr}} \right) \times 100 \ldots\ldots\ldots\ldots\ldots\ldots (1)$$

The area of the part covered by the damper (θ) was calculated according to equation (2):

$$\theta = \frac{\text{I°corr} - \text{Icorr}}{\text{Icorr}} \ldots\ldots\ldots\ldots\ldots\ldots (2)$$

It is seen that the upsides of the corrosion current densities for the clear arrangement of plant extracts utilized as inhibitors are more prominent than the upsides of the corrosion current densities within the sight of inhibitors with the temperature steady, where I1corr and Icorr address the corrosion current densities in the nonappearance and presence of the inhibitor, separately. At each temperature, the corrosion current thickness drops as the inhibitor fixation rises, proposing that the expansion of the inhibitor hinders the corrosion attack. This suggests that the corrosion attack is blocked by the consideration of an inhibitor. At the point when an inhibitor is added, there are anodic and cathodic curves, however the anodic bend has a fairly more extreme incline than the cathodic bend. This demonstrates that the expansion of inhibitors modifies the energy of the hydrogen discharge process as well as the disintegration response of carbon steel. The crumbling of steel is the variable generally affected. The degrees of βa and βc can likewise differ because of the contribution of different sorts of negative particles in the arrangement during the adsorption cycle. [15].

(b) Corrosion Rate (CR)

The units of measurement for the rate of corrosion speed (CR) in an acidic medium with varying quantities of plant extract acting as an inhibitor and at temperatures between (298,308, 318) K

Using the connection, the corrosion speed rate (CR) value was computed. (3) [16]:

$$\text{CR} = \text{K} \times \frac{\text{Icorr}}{\rho} \times \text{E.W} \ldots\ldots\ldots\ldots\ldots\ldots (3)$$

It represents:

CR/corrosion rate in units (mpy).

I_{corr} /corrosion current density in the presence of the inhibitor in units ($\mu A/Cm^2$).

EW / equivalent weight of metal or alloy (E. WFe =27.8 gm / mol).

ρ /density of the metal or alloy (ρFe = 7.86 g/cm3)

K / constant value equal to (0.1288 mpy g / μA cm).

Equation (3) illustrates how the corrosion current density Icorr and corrosion speed CR are related. The dissolution of the metal during the anodic reaction is the cause of the relatively high rate of corrosion speed (CR) in the absence of inhibitors, as Table (4) demonstrates.

Because the inhibitor lowers the corrosion current on the alloy's surface, the rate of corrosion of the carbon steel alloy is slowed down [17].Furthermore, we discover that, when the concentration of the plant inhibitor R used at constant temperature increases, the rate of corrosion speed (CR) decreases; conversely, when temperature rises and concentration remains constant, the rate of corrosion speed (CR) increases because of the weak physical adsorption's collapse towards rising temperatures [18].

(c) Effect of Temperature

The results of inhibition efficiency (%IE) and corrosion speed rate (CR) installed can be summarized in Table 4 and Figure 6 as follows:

(1) As was indicated at the conclusion of the preceding paragraph, corrosion rate (CR) values increase with increasing temperature and decrease with increasing inhibitor concentration.

(2) For the same concentration, the values of inhibitory efficiency %IE drop as temperature rises. As the concentration of the inhibitor reaches a stable temperature, it rises. The reason for this could be that the inhibitor's physical adsorption process on carbon steel's surface, which prefers a lower temperature, causes the inhibition efficiency to drop with increasing temperature. While in chemisorption the inhibitory efficiency rises with temperature. [19]

Table (4) Polarization curve data for the corrosion of carbon steel alloy at different inhibitor (R) concentrations in a solution of hydrochloric acid (1 M) and in the temperature range of 298-318

Temp (K)	Inhibitor Conc(ppm)	E_{corr} (mV)	CR (mpy)	Icorr ($\mu A/Cm^2$)	βa (mv/Dec)	βc (mv/Dec)	% IE	θ
298	Blank	-439.1	15.58	34.22	105.7	-128.6	0	0
308		-449.0	18.92	41.54	113.2	-159.1	0	0
318		-449.3	22.39	49.15	80.5	- 59.4	0	0
298	50 ppm	-419.2	5.97	13.11	83.5	-155.2	61.68	0.61
308		- 408.8	8.82	19.37	105.0	-117.4	53.37	0.53
318		- 429	12.04	26.43	78.8	-159.6	46.22	0.46
298	100 ppm	-388.7	4.67	10.26	80.2	-146.8	70.01	0.70
308		- 418.9	7.27	15.97	80.4	-142.5	61.55	0.61
318		- 429.0	10.90	23.94	87.3	-135.2	51.23	0.51
298		-408.8	3.47	7.62	78.3	-163.5	77.73	0.77

308	150 ppm	-409	5.32	11.7	76.7	-147.8	71.83	0.71
318		-349.6	7.77	17.07	86.2	-180.1	65.26	0.65
298	200 ppm	-428.9	1.36	2.99	63.9	-115.6	91.26	0.91
308		-408.4	2.66	5.84	56.9	-118.4	85.94	0.85
318		-418.9	3.91	8.59	53.1	-128.9	82.52	0.82

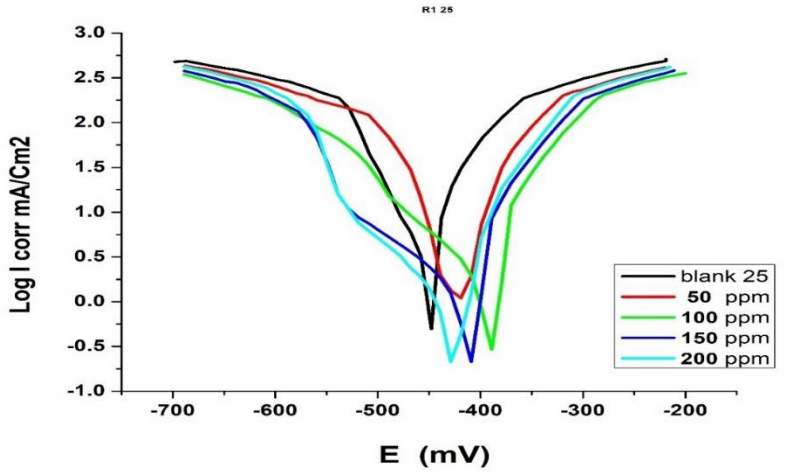

Figure (3): Polarization curves for carbon steel corrosion at 298 K with varying inhibitor (R) concentrations

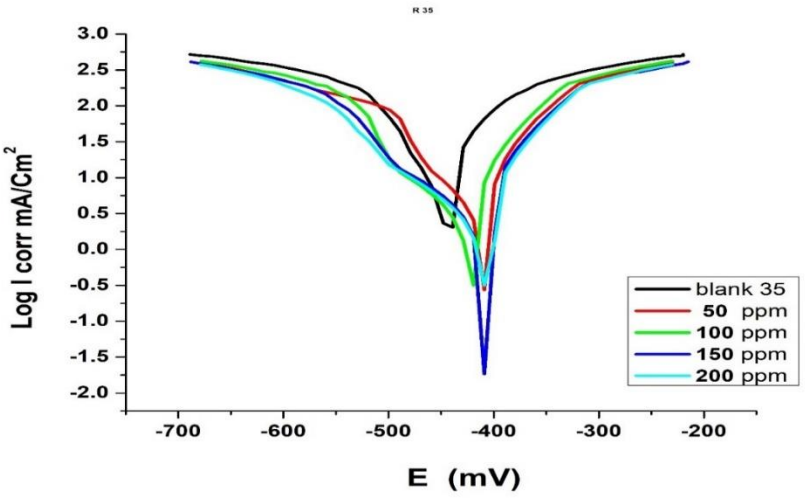

Figure (4): Polarization curves for carbon steel corrosion at 308 K with varying inhibitor (R) concentrations

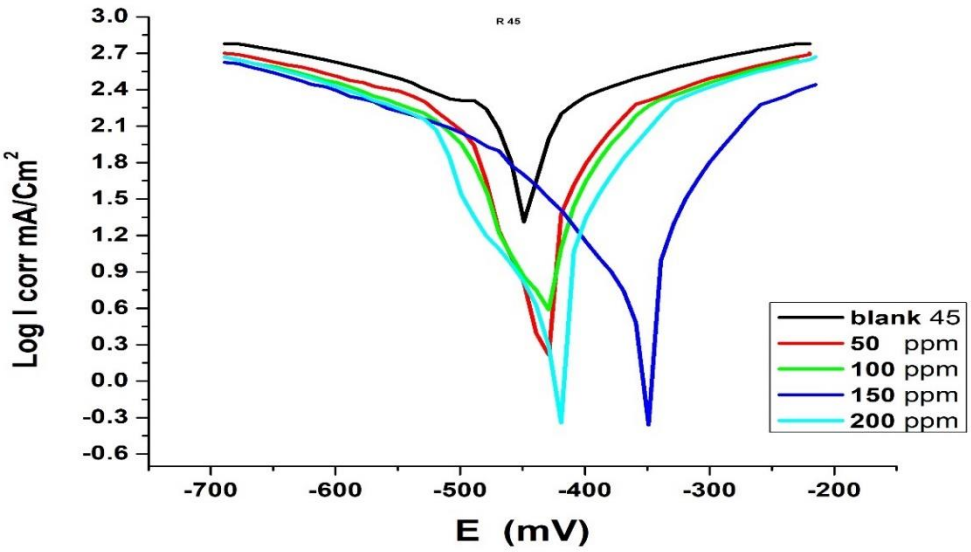

Figure (5): Polarization curves for carbon steel corrosion at 318 K with varying inhibitor (R) concentrations

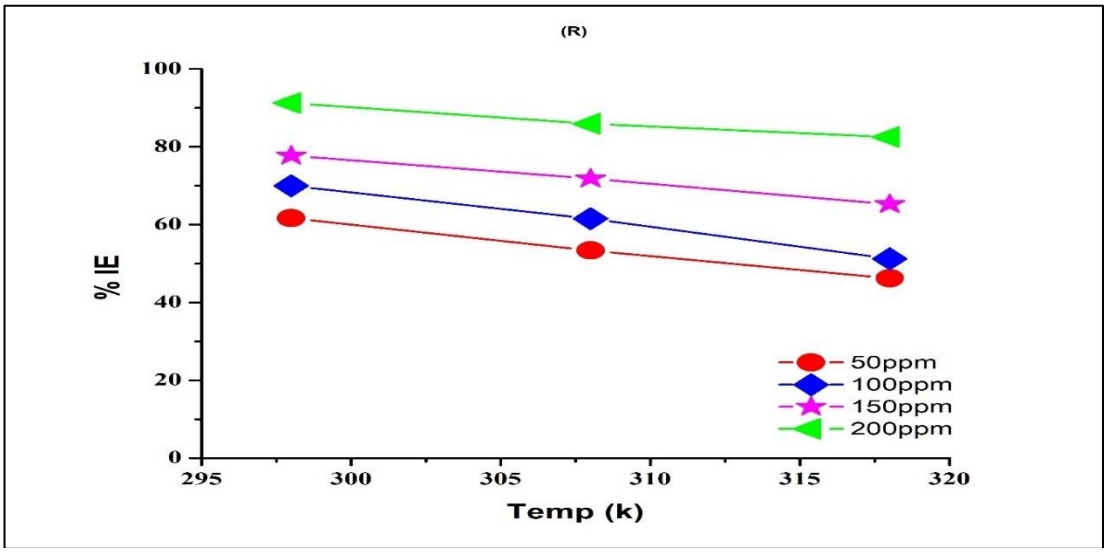

Figure (6): The correlation between temperature and inhibition efficiency for a variety of temperatures (298 – 318 K) and acidic solutions with varying inhibitor (R) concentrations

(d) Study of the kinetic variables of the corrosion process

For a carbon steel composite in a destructive hydrochloric corrosive medium at a grouping of (1M), the energy of the corrosion response were followed, and the effect of temperature was explored both in the presence and nonappearance of the inhibitor (R) and at explicit focuses.

To understand how the specific inhibitor adsorbed on the alloy surface and how strong it was, a number of kinetic functions for the adsorption process were also computed. Using the Arnos equation as a basis, the relationship between temperature and corrosion speed was investigated within the experimental temperature range. (4) [20].

$$\text{Log Icorr} = \text{Log A} - \frac{\text{Ea}}{2.303\ \text{RT}} \dots\dots\dots\dots\dots\dots\dots (4)$$

where Arrhenius constant (A), activation energy (Ea), temperature (T), gas constant (R), and corrosion current (Icorr) are represented. A straight line results from plotting the values of Log Icorr against the values of 1/T, as shown in Figure (7), where the linear relationship's intercept is (Log A) and its slope is (-Ea/(2.303 R)). Utilizing Equation (4) as Discover the activation energy (Ea), as it will be necessary to determine additional kinetic functions.

The kinetic functions of the activated complex, such as the entropy of activation ($\Delta S^{\ddagger}$) and the enthalpy of activation ($\Delta H^{\ddagger}$), were determined from the transition state equation (5) [21]. These values provide information about how the activated complex is created for the corrosion process in acidic media.

$$\text{Log}\ \frac{\text{Icorr}}{\text{T}} = \text{Log}\ \frac{\text{R}}{\text{N h}} + \left(\frac{\Delta S^{*}}{2.303}\right) - \left(\frac{\Delta H^{*}}{2.303\ \text{RT}}\right) \dots\dots\dots\dots\dots\dots\dots (5)$$

The value of (ΔH *) is found by the linear connection shown in Figure (8), whose cut-off is [(Log R/hN) + (ΔS^{*}) / (2.303 R)]. The slope of this relationship is (-ΔH^{*}/ (2.303 R)). Equation can be used to derive $\Delta G^{\ddagger}$ by determining the value of (ΔS*) once the values of (ΔS *) and (ΔH *) have been determined. (6) [22].

$\Delta G^{*} = \Delta H^{*} - T\ \Delta S^{*} \dots\dots\dots\dots$ ..(6)

As an expansion in actuation energy (Ea.) is seen, Table (5) shows the upsides of (Ea.), (ΔS*), (ΔH*), and (ΔG*) for the corrosion of carbon steel in hydrochloric corrosive (1M) in the presence and nonattendance of the inhibitor. Physical (electrostatic) factors oversee the corrosion cycle when the inhibitor is available rather than when it isn't, making sense of the improvement of a flimsy layer of inhibitor that is adsorbed on the outer layer of the combination being used [23]. This is reliable with the possibility that actual adsorption happens in the main stage, trailed by the desorption cycle, as the effectiveness of hindrance diminishes with climbing temperature. scientist [24]. Enthalpy of enactment ($\Delta H^{\ddagger}$) values that are positive additionally propose that the response is endothermic and that it strengthens when the inhibitor's fixation ascends in contrast with when it is missing. This shows that the breaking down process is testing and that the response of cardboard steel in hydrochloric corrosive (1M) is spongy [25]. Within the sight of the inhibitor, the initiation entropy ($\Delta S^{\ddagger}$) might be more noteworthy and more negative. This worth develops with fixation, recommending that the reactants adsorb less haphazardly and become dynamic edifices adsorbed on the carbon steel combination's surface. The hard free energy of adsorption (ΔG*) has high and positive qualities, demonstrating that the corrosion cycle on the combination isn't unconstrained. [26].

Table (5): The values of a few kinetic functions (ΔG^{*}, ΔH^{*}, ΔS^{*}, and Ea) in acidic environments and between 298 and 318 K with and without varying inhibitor (R) concentrations

Comp.	Conc.	Ea. (KJ.mol-1)	ΔS* (KJ. mol-1. K-1)	Δ H* (KJ.mol-1)	Δ G* (KJ.mol-1) 298 K	K 308	318 K
HCL	1 M	14.27	-0.18	11.71	64.20	66	67.80
R	50 ppm	27.65	-0.14	25.09	66.59	67.99	69.38
	100ppm	33.39	-0.12	30.83	67.22	67.95	70.18
	150ppm	31.79	-0.13	29.23	68.44	69.25	71.22
	200ppm	41.68	-0.10	39.12	69.66	70.55	72.26

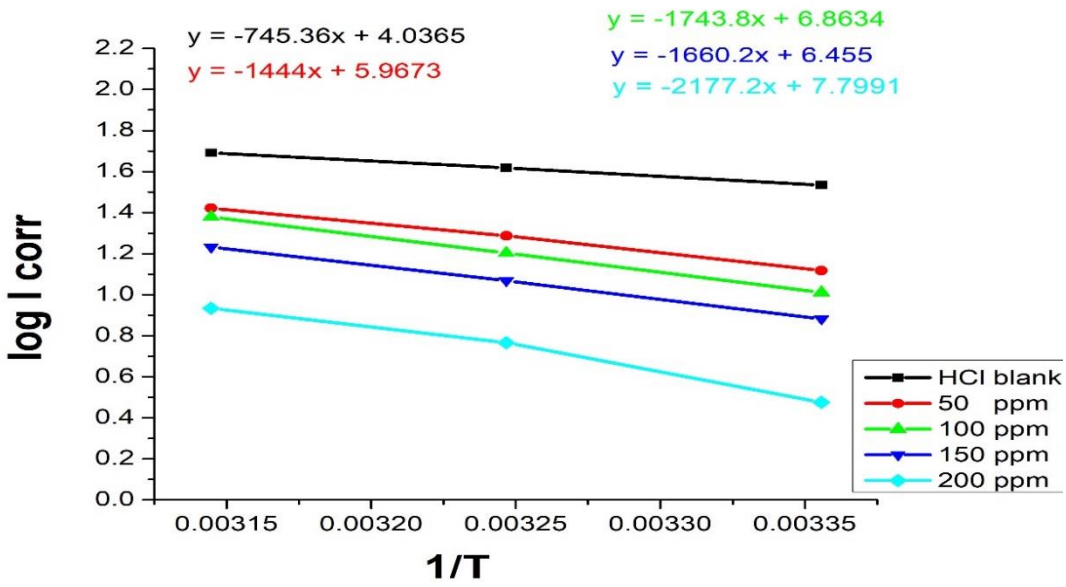

Figure (7): Arrhenius relationship in the temperature range (298-318 K) and in the presence and absence of the inhibitor (R).

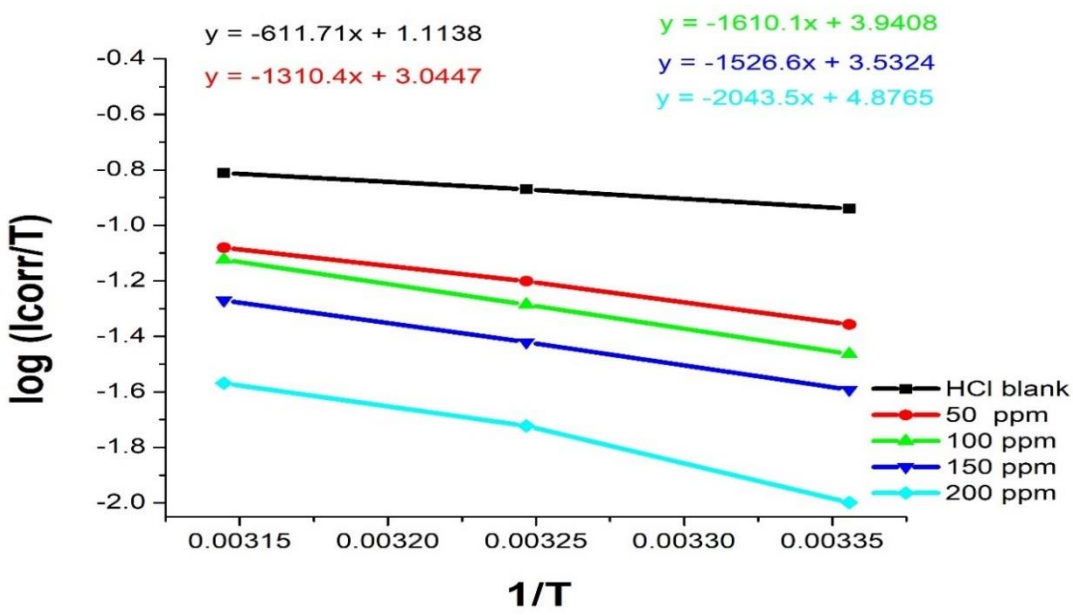

Figure (8): The connection between the transition state and the enthalpy and entropy calculations within the temperature range (298-318 K) and in the presence and absence of the inhibitor (R)

3.4 Analysis of the carbon steel alloy's surface morphology with a Spectrometer Scanning Electron Microscope (SEM).

The morphological adjustments on the carbon steel combination's surface were noticed utilizing scanning electron microscopy (SEM) gear. The best convergence of inhibitor (200 PPM) at a temperature of 25°C for an hour of drenching is available in the SEM tiny pictures of the carbon steel surface, which were gotten after the material was presented to an acidic medium that isn't destructive. The outer layer of the carbon steel amalgam is smooth and liberated from harm or disfigurement when the acidic medium is missing. On the other hand, in the case of microscopic image No. (b), which represents the situation where the corrosive medium is present but inhibitors are absent, we observe significant damage and deformation due to HCl acid corrosion, as demonstrated by the smooth surface of microscopic image No. (C) in Figure (9), which represents the situation where the inhibitor (R) is present. This is explained by the thin layer of protection it forms and its high level of protection. due to inhibitors adhering to the surface of carbon steel either chemically or physically.

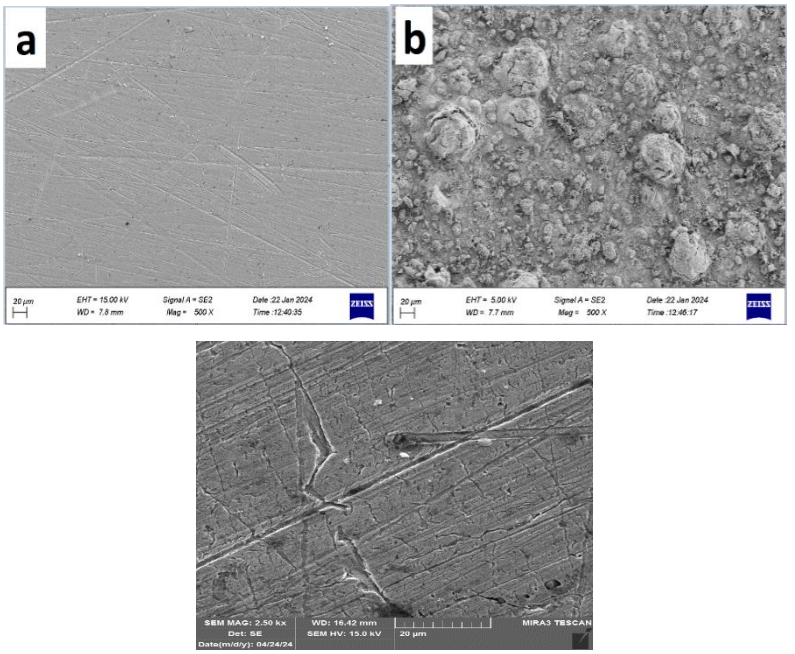

Figure (9): In each of the three scenarios, technical images (SEM) of carbon steel

3.5 Mechanism of action of inhibitors

Some aqueous plant extracts prevent the dissociation reaction of metals immersed in the corrosive medium. The reason for this inhibitory performance is that it contains organic compounds known for their ability to suppress corrosion by adsorbing them on the surface of the metal, forming an insulating layer. Due to the presence of atoms or groups with high electrical negativity, these materials become effective. The compounds under study may contain atoms (N, O, S) or groups (C=N, N=N, C=C) in addition to the presence of a π system, which is an electron provided by the aromatic rings. Therefore, one of the following plausible paths could explain the mechanism of inhibiting chemicals under study [27]:

1. The possibility of the aromatic ring of the inhibitor interacting with the atoms of the metal surface, causing the π electrons to interfere with the d orbitals of the metal surface, thus forming a shield on the metal surface that prevents corrosive substances from penetrating it and slows down the chemical corrosion process [28], as in Figure 10.

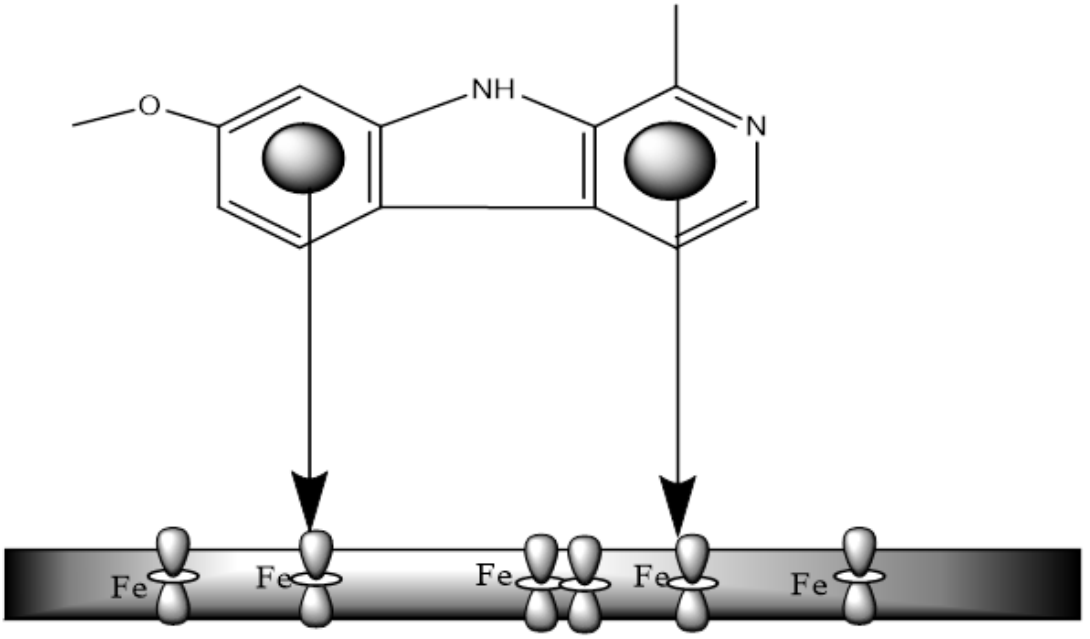

Figure (10): One of the inhibitor compounds (R), harmine, exhibits interference with the d-orbitals of the iron atoms through the aromatic ring's π electrons.

2. The potential for the plant inhibitor to chemically adsorb onto the metal's surface via the interference of free electronic pairs on nitrogen (N) and oxygen (O) atoms with the metal's partially or fully filled d-orbitals via ionic, covalent, or coordination bonds. As a result, the inhibitor molecules adhere to the surface. As seen in Figure 11, the alloy thereby keeps the corrosive liquid from reaching it, decreasing chemical corrosion [29].

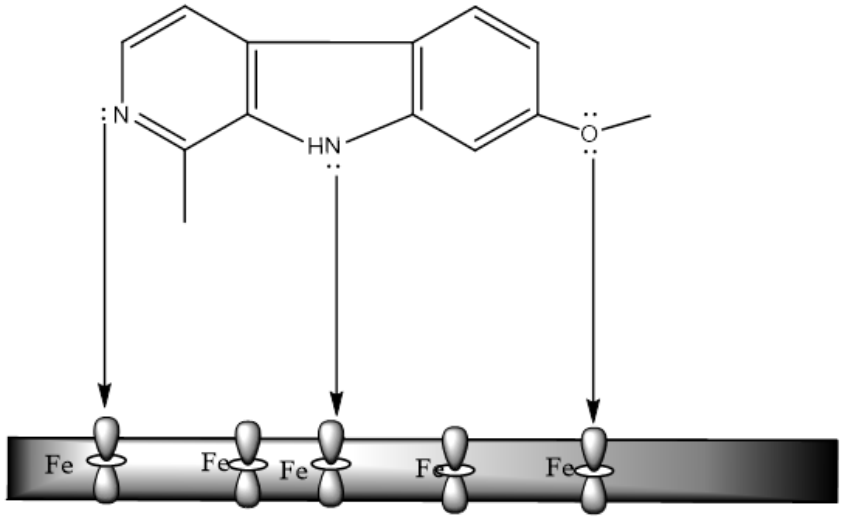

Figure (11): Interference between the d-orbitals of the iron atoms and the free electronic pairs on the oxygen (O) and nitrogen (N) atoms in the molecule harmine, one of the inhibitor

compounds (R).

4. Conclusions

In the acidic medium HCL 1M, the inhibitor (R) stops N80 carbon steel from corroding. According to the outcomes of the electrochemical tests, (R) can be applied to N80 carbon steel to prevent corrosion. At 200 PPM concentration and 298 K, the greatest rate of inhibition was observed. Moreover, the electrochemical test discoveries demonstrated that the proficiency of hindrance improves with expanding inhibitor focus and declines with increasing temperature (R).

References

1. X. Yue, L. Zhang, H. Liu, H. Zhao, S. Wang, Y. Hua, Uncoupling chloride and acidification attack on the naturally formed corrosion scales, Corros. Sci. 199 (2022) 110207. https://doi.org/10.1016/J.CORSCI.2022.110207.
2. A.M. Farhan, R.A. Jassim, N.J. Kadhim, W.A. Mehdi, A.A. Mehde, Synthesis of Silver Nanoparticles from Malva parviflora extract and effect on Ecto-5'-Nucleotidase (5'-NT), ADA and AMPDA enzymes in sera of patients with arthrosclerosis, Baghdad Sci. J. 14 (2017) 742.
3. M.N. Rahuma, M.B. EL-Sabbah, I.M. Hamad, Effect of serine and methionine on electrochemical behavior of the corrosion of mild steel in aqueous solutions, Int. Sch. Res. Not. 2013 (2013).
4. A. Sedik, D. Lerari, A. Salci, S. Athmani, K. Bachari, İ.H. Gecibesler, R. Solmaz, Dardagan Fruit extract as eco-friendly corrosion inhibitor for mild steel in 1 M HCl: Electrochemical and surface morphological studies, J. Taiwan Inst. Chem. Eng. 107 (2020) 189–200.
5. A. Saxena, D. Prasad, R. Haldhar, Investigation of corrosion inhibition effect and adsorption activities of Cuscuta reflexa extract for mild steel in 0.5 M H2SO4, Bioelectrochemistry 124 (2018) 156–164.
6. M. Toorani, M. Aliofkhazraei, M. Mahdavian, R. Naderi, Superior corrosion protection and adhesion strength of epoxy coating applied on AZ31 magnesium alloy pre-treated by PEO/Silane with inorganic and organic corrosion inhibitors, Corros. Sci. 178 (2021) 109065.
7. Mushtaq J. Meften ; Wisam A. Radhi and Atheer N. Abulhail, Molecular structure and electronic characteristics study of imidazole and dioxol derivatives as corrosion inhibitors . A quantum methodology investigation ., Basrah J. Sci. (C) 36 (2018) 1–29. https://doi.org/10.29072/basjs.2018302.
8. M.H. Shahrajabian, W. Sun, Q. Cheng, Improving health benefits with considering traditional and modern health benefits of Peganum harmala, Clin. Phytoscience 7 (2021) 1–9.
9. M.H. Yusoff, M.N. Azmi, M.H. Hussin, H. Osman, P.B. Raja, A.A. Rahim, K. Awang, An Electrochemical evaluation of synthesized coumarin-Azo dyes as potential corrosion inhibitors for mild steel in 1 M Hcl medium, Int. J. Electrochem. Sci. 15 (2020) 11742–11756.
10. N. Agyepong, C. Agyare, M. Adarkwa-Yiadom, S.Y. Gbedema, Phytochemical investigation and anti-microbial activity of Clausena anisata (Willd), Hook., African J. Tradit. Complement. Altern. Med. 11 (2014) 200–209.
11. B.M. Praveen, B.M. Prasanna, N.M. Mallikarjuna, M.R. Jagadeesh, N. Hebbar, D. Rashmi, Investigation of anticorrosive behaviour of novel tert-butyl 4-[(4-methyl phenyl) carbonyl] piperazine-1-carboxylate for carbon steel in 1M HCl, Heliyon 7 (2021).
12. S. Deng, X. Li, H. Fu, Alizarin violet 3B as a novel corrosion inhibitor for steel in HCl, H2SO4

solutions, Corros. Sci. 53 (2011) 3596–3602.
13. R. Lopes-Sesenes, G.F. Dominguez-Patiño, J.G. Gonzalez-Rodriguez, J. Uruchurtu-Chavarin, Effect of flowing conditions on the corrosion inhibition of carbon steel by extract of buddleia perfoliata, Int. J. Electrochem. Sci. 8 (2013) 477–489.
14. R.H. Tammam, A.M. Fekry, M.M. Saleh, Understanding different inhibition actions of surfactants for mild steel corrosion in acid solution, Int. J. Electrochem. Sci 11 (2016) 1310–1326.
15. C. Verma, E.E. Ebenso, I. Bahadur, M.A. Quraishi, An overview on plant extracts as environmental sustainable and green corrosion inhibitors for metals and alloys in aggressive corrosive media, J. Mol. Liq. 266 (2018) 577–590.
16. E.M. Attia, Dipron: an eco-friendly corrosion inhibitor for iron in HCl media in both micro and nano scale particle size-Comparative study, Int. J. Adv. Res 4 (2016) 986–1003.
17. I. Hamdani, E. El Ouariachi, O. Mokhtari, A. Salhi, A. Bouyanzer, A. Zarrouk, B. Hammouti, J. Costa, An investigation of mild steel corrosion inhibition in hydrochloric acid medium by environment friendly green inhibitor, Sch. Res. Libr. Der Pharm. Lett. 7 (2015) 109–118.
18. M. Manssouri, Y. El Ouadi, M. Znini, J. Costa, A. Bouyanzer, J.M. Desjobert, L. Majidi, Adsorption proprieties and inhibition of mild steel corrosion in HCl solution by the essential oil from fruit of Moroccan Ammodaucus leucotrichus, J. Mater. Environ. Sci 6 (2015) 631–646.
19. A.M. Al-Sabagh, N.G. Kandil, O. Ramadan, N.M. Amer, R. Mansour, E.A. Khamis, Novel cationic surfactants from fatty acids and their corrosion inhibition efficiency for carbon steel pipelines in 1 M HCl, Egypt. J. Pet. 20 (2011) 47–57.
20. A. Al Bahir, Estimation of the performances of creatine and creatinine as eco-friendly corrosion inhibitors for copper in sodium hydroxide solution, Int. J. Electrochem. Sci. 18 (2023) 100040.
21. M.A. Quraishi, A. Singh, V.K. Singh, D.K. Yadav, A.K. Singh, Green approach to corrosion inhibition of mild steel in hydrochloric acid and sulphuric acid solutions by the extract of Murraya koenigii leaves, Mater. Chem. Phys. 122 (2010) 114–122.
22. A. Toghan, A. Fawzy, A. Al Bahir, N. Alqarni, M.M.S. Sanad, M. Khairy, A.I. Alakhras, A.A. Farag, Computational foretelling and experimental implementation of the performance of polyacrylic acid and polyacrylamide polymers as eco-friendly corrosion inhibitors for copper in nitric acid, Polymers (Basel). 14 (2022) 4802.
23. T. Szauer, A. Brandt, Adsorption of oleates of various amines on iron in acidic solution, Electrochim. Acta 26 (1981) 1253–1256.
24. T. Douadi, H. Hamani, D. Daoud, M. Al-Noaimi, S. Chafaa, Effect of temperature and hydrodynamic conditions on corrosion inhibition of an azomethine compounds for mild steel in 1 M HCl solution, J. Taiwan Inst. Chem. Eng. 71 (2017) 388–404.
25. V.R. Saliyan, A.V. Adhikari, Quinolin-5-ylmethylene-3-{[8-(trifluoromethyl) quinolin-4-yl] thio} propanohydrazide as an effective inhibitor of mild steel corrosion in HCl solution, Corros. Sci. 50 (2008) 55–61.
26. A.K. Singh, M.A. Quraishi, Effect of 2, 2′ benzothiazolyl disulfide on the corrosion of mild steel in acid media, Corros. Sci. 51 (2009) 2752–2760.
27. H.M. Abd El-Lateef, M. Ismael, I.M.A. Mohamed, Novel Schiff base amino acid as corrosion inhibitors for carbon steel in CO2-saturated 3.5% NaCl solution: experimental and computational study, Corros. Rev. 33 (2015) 77–97.
28. D.S. Chauhan, M.A.J. Mazumder, M.A. Quraishi, K.R. Ansari, Chitosan-cinnamaldehyde Schiff base: A bioinspired macromolecule as corrosion inhibitor for oil and gas industry, Int. J. Biol. Macromol. 158 (2020) 127–138.
29. M.Y. Kadhim, A.M. Abdulsada, J.M.S. Alshawi, Synthesis, identification and the study of some new azo dyes as corrosion inhibitors for copper in (1m) HCl, J. Basrah Res. 40 (2014).